 Bull. Chem. Soc. Jpn., 76, 663–672 (2003)

Molecular Orientation in the Organized Molecular Films of Fluorinated Comb Polymers with Various Chain Lengths Studied by Soft X-ray Absorption Spectroscopy

Atsuhiro Fujimori, Tohru Araki,[#] Hiroo Nakahara,[*] Eisuke Ito,[†] Masahiko Hara,[†] Noritaka Matsuie,[††] Hisao Ishii,[††] Yukio Ouchi,[††] and Kazuhiko Seki[†††,##]

Department of Chemistry, Faculty of Science, Saitama University, Shimo-okubo 255, Saitama 338-8570

†Local Spatio-Temporal Function, Frontier research system, The Institute of physical and chemical research (RIKEN), Hirosawa 2-1, Wako, 351-0198

††Department of Chemistry, Graduate School of Science, Nagoya University, Furo-cho, Chikusa-ku, Nagoya 464-8602

†††Research Center for Materials Science, Nagoya University, Furo-cho, Chikusa-ku, Nagoya 464-8602

(Received September 24, 2002)

The molecular orientation in multilayer films of fluorinated comb polymers with various side-chain lengths can be characterized by near-edge X-ray absorption fine structures (NEXAFS) spectroscopy at the C K- and F K-edges. The spectra are found to change significantly with respect to the incidence angles of the soft X-rays and the number of layers in organized molecular films as well as chemical modifications such as fluorocarbon side-chain lengths, the atoms at the ω-position of the fluorocarbon side-chains, and α-methyl substituents. Analysis of these changes of the NEXAFS spectra provides useful information about the average molecular orientation in the X- and Z-types of mono- and multilayer films of the fluorinated comb polymers on solids.

Fluorinated polymers and amphiphiles have been already used practically in thin films thanks to their physical behavior of low friction coefficient[1,2] and chemical-resistance. The molecular orientations of fluorocarbon chains, in addition to the characteristics of a large van der Waals radius and electronegativity of the fluorin atom, seem to be indispensable to such functions.[3] Fluorocarbon chains $-(CF_2-CF_2)_n-$ of poly(tetrafluoroethylene)[3,4,5] take some helical conformations with rigid rod-like forms which are clearly different from the normal hydrocarbon chains with the *trans* zig-zag planar structure. For fabrication of well-defined molecular alignments controlled at the monomolecular level, the monolayer assemblying method could be applied to the fluorinated comb polymers. Structural characterizations of those films have been carried out using the in situ Brewster angle microscopy, the scanning electron microscopy, the atomic force and friction force microscopies (AFM and FFM) and both the out-of and in-plane X-ray diffractions.[6,7,8]

Furthermore, for the purpose of clarifying the molecular orientation of the fluorinated comb polymers in the organized molecular films, researches have applied the near-edge X-ray absorption fine structure (NEXAFS) spectroscopy with polarized continuous light in the soft X-ray region. In general, the NEXAFS spectra can be expected to give the information about binding energies and short-ranged lattice structures of the constituent elements in surface region of solids by utilizing the short mean free path of released photoelectrons, such as a partial electron yield (PEY) mode.[9,10] Previously, orientation of hydrocarbons in the Langmuir–Blodgett (LB) films of cadmium arachidate[11] and the photopolymerization of a long-chain diacetylene derivative in LB films[12] have been elucidated and discussed by using the angular dependence of the incident X-ray on the NEXAFS spectra, and by referring to the observations of the ultraviolet photoelectron spectroscopy (UPS), respectively. It is expected that the NEXAFS spectroscopy has a preference to fluorine compounds with a relatively large scattering power of photoelectrons.

In previous reports, oriented perfluorotetracosane [n-CF_3-$(CF_2)_{22}CF_3$] and poly(tetrafluoroethylene) [PTFE, $(-CF_2-)_n$] evaporated films have been studied by polarized NEXAFS spectroscopy.[13–15] Recently, a study that compared the experimental NEXAFS spectra with the ones calculated for the rubbed PTFE film, was reported by Castner et al.[16] Furthermore, molecular alignments of n-alkane multilayers on alkanethiolate monolayers and the structure of self-assembled films of octadecyltrichlorosilane have been investigated by soft X-ray absorption spectroscopy.[17,18] Structural studies of electrodeposited iridium oxide films in aqueous electrolytes have also carried out by in situ X-ray absorption spectroscopy.[19] As the primary result of a part of this work, we reported the characterization of organized molecular films of the fluorinated comb polymers with the polarized NEXAFS spectroscopy at F

Present address: Department of Chemistry, Brockhouse Institute for Materials Research, McMaster University, 1280 Main St. W., Hamilton, Ontario, Canada L8S 4M1

Department of Chemistry, Graduate School of Science, Nagoya University

K-edge.[20] In this investigation, the molecular alignments in the transferred films of the comb polymers with fluorocarbon side-chains having various lengths and different atoms at the ω-position are investigated by NEXAFS spectroscopy at both C K- and F K-edges for the X- and Z-types of mono- and multilayer films on solids. We have also studied the effects of hydrogen bonding to introduce the disordering molecular arrangement, depending on various spreading solvents and on the number of layers. The curve fitting of the asymmetric peaks of NEXAFS spectra and their dependence of the incidence angles for the films of fluorinated comb polymers were analyzed to obtain the orientation of the fluorocarbon side-chains, assuming their uniaxial orientation.

Experimental

Materials. Table 1 shows fluorinated amphiphiles with vinyl groups as monomer materials, 2-(perfluoroalkyl)ethyl acrylate and methacrylate, $F(CF_2)_nCH_2CH_2OCOC(X)=CH_2$ [n = 6, 8, and 10; abbreviated as FF_nEA and FF_nEMA for X = –H and $–CH_3$, respectively], and also 1H, 1H, 11H-icosafluoroalkyl acrylate and methacrylate, $H(CF_2)_nCH_2OCOC(X)=CH_2$, [$n$ = 4, 6, 8, and 10; abbreviated as F_nA and F_nMA for Z = –H and $–CH_3$, respectively]. These were purchased from Daikin Fine Chemicals Co. Ltd. and purified by recrystallizations repeated several times from *n*-hexane solutions. These analogous monomers containing the fluorocarbons with various chain-lengths sealed in Pyrex glass tubes in a vacuum were irradiated with ^{60}Co γ-rays (1.0 Mrad in liq.-N_2) at -196 °C, and the post-polymerization treatments were carried out in the range of $-83 \sim 50$ °C. The obtained comb polymers were dissolved in a little acetone or tetrahydrofuran and purified by precipitation through pouring into tetrachloromethane.[21,22] These fluorinated comb polymers were practically insoluble in common organic solvents without trifluoroacetic acid. The tacticity of these polymers was obtained to be almost syndiotactic (Diad: 57.4%) by ^{1}H-NMR analysis according to the reference.[23] Their molecular weights were estimated to be $1.5–6.0 \times 10^4$ from the intrinsic viscosity of $[\eta] = 0.12–0.54$ for these trifluoroacetic acid solutions at 30 °C. Chemical structures of these fluorinated comb polymers are also indicated in Table 1, together with the abbreviations of Poly-FF_nEA, Poly-FF_nEMA [n = 6, 8, and 10], Poly-F_nA, and Poly-F_nMA [n = 4, 6, 8, and 10].

Procedures. These samples were dissolved in trifluoroacetic acid as a good solvent. The monolayers were spread on the distilled water surface (Milli-Q Plus, 18.2 MΩcm) to allow the solution to flow down along a small glass rod projecting from the surface of the aqueous subphase into a trough, according to the method suggested by Trurnit.[24] These monolayers were transferred onto NESA glass substrates at 5 °C by a horizontal lifting[25] and a surface-lowering method[26] at various surface pressures to obtain the non-alternating X- and Z-type films, respectively. It is considered that the polymer skeletons and the fluorocarbon side-chains are exposed to the air in the outermost surfaces of the X- and the Z-type films, respectively. NEXAFS spectra were measured on the BL-7A and -11A soft X-ray beamlines at the parallel-polarized, grazing incidence monochromator station of the Photon Factory in the National Laboratory for High-Energy Accelerator Research Organization (KEK-PF) with synchrotron radiation from a bending-magnet source.[27,28] The F K-edge and C K-edge spectra were measured in the photon energy regions of 660–760 eV and 275–325 eV, and in the partial electron yield mode (PEY) with -450 and -200 V retarding voltages, respectively and 2.0 kV accelerating voltage under the vacuum of 10^{-8} Torr. The optimization of the retarding voltages at both edges was carried out for every sample. These conditions could provide the clear NEXAFS spectra that contain the structural information of the top few layers of the multilayer films by considering the probing depth about 50 Å, as illustrated by Scheme 1.[9] The resolution of the spectra was

Table 1. Fluorinated Amphiphilic Vinyl Monomers of Acrylate and Methacrylate and Those Comb Polymers Containing Fluorocarbons as the Side-Chains Used in This Work, Together with Their Abbreviation

		Abbrev.	length
Monomers			
$F(CF_2)_nCH_2CH_2OCOC(X)=CH_2$	X = H	FF_nEA	
2-(perfluoroalkyl)ethyl	acrylate		
	X = CH_3	FF_nEMA	
	methacrylate		
$H(CF_2)_nCH_2OCOC(X)=CH_2$	X = H	F_nA	
1H, 1H, (n + 1)H-partialfluoroalkyl	acrylate		
	X = CH_3	F_nMA	
	methacrylate		
Comb polymers			
$[OC(F(CF_2)_nCH_2CH_2O)C(X)-CH_2]_m$	X = H	Poly-FF_nEA	
Poly-2-(perfluoroalkyl)ethyl	acrylate		n = 6,8,10
	X = CH_3	Poly-FF_nEMA	
	methacrylate		
$[OC(H(CF_2)_nCH_2O)C(X)-CH_2]_m$	X = H	Poly-F_nA	
Poly-1H, 1H, (n + 1)H-(partialfluoroalkyl)	acrylate		n = 4,6,8,10
	X = CH_3	Poly-F_nMA	
	methacrylate		

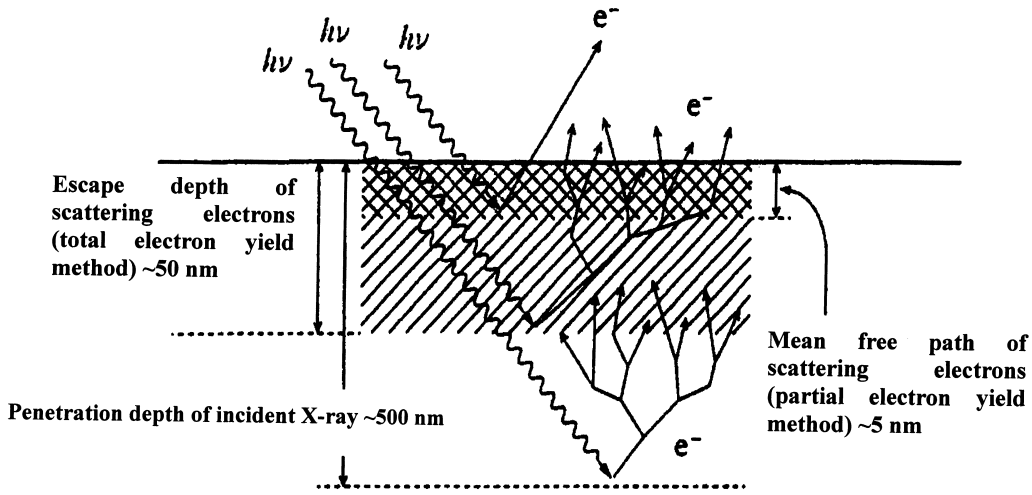

Scheme 1. Mean free path of scattering electrons with the soft X-ray absorption of organic thin films.

Table 2. Standard Samples

Edge	Standard samples	Peak position[10,13]
C K	Hexatriacontane (HTC)	287.80 eV (C1s–σ^*(C–H) transition)
F K	Perfluorotetracosane (PFT)	693.97 eV (F1s–σ^*(C–F) transition)

0.3 eV at the C K-edge. The NEXAFS spectra were measured without any pre-annealing and no contribution from the substrate of NESA glass could be detected. In addition, no drastic structural changes such as bonding scission[29] of fluorocarbons could be found from IR spectroscopy and X-ray diffraction results taken before and after the measurements of NEXAFS spectra.

Analytical Procedures of NEXAFS Spectra. a. Correction of Photon Energies on the X-Axis: From the measurements of the polarized NEXAFS spectra for the standard samples of oriented films deposited by evaporation at magic angle on several edges (Table 2), the energy on the X-axis was corrected by the obvious peak positions.

b. Normalization of Spectral Intensity on the Y-Axis: The relative intensities of every peaks in NEXAFS spectra were corrected for variation of the incident angles accompanying changes of the probing area on the sample. The changes of the peak intensity with decrease of the ring current were normalized by the edge-jump, which corresponds to the transition to the continuous state in higher energy region than vacuum level, that is, the difference of the base lines before and after the absorption bands of spectra.

From the angular dependence of the normalized intensity of NEXAFS spectra plotted against the incident angles, it is possible to compare and discuss the order of molecular orientation, depending upon the film types and the chemical modification.

c. Spectral Analysis (Curve Fitting) of NEXAFS Spectra: According to the literature,[9,11] the obtained NEXAFS spectra were deconvoluted by fitting the following Gaussian function from the lower to the high photon energies. The Gaussian equation was expressed by the following I_g:

$$I_g = H \times \exp\{-1/2[(E - P)/(\Gamma/c)]^2\} \quad (1)$$

where $\Gamma = E \times m + b$ (antisymmetric parameters m and b were constants), E is a photon energy near the resonance (generally from zero values at the peak position of the step), H is a peak height, P is the peak position, and $c = 2 \times (\ln 4)^{1/2} = 2.355$, respectively.

d. Determination of the Molecular Orientation Angle: The orientation angles of fluorocarbon side-chains for several comb polymers in the films were determined by comparison of the polarized dependence of the peak intensities for the NEXAFS spectra with the calculations based on the following uniaxial molecular orientation in the films.[29,30] In contrast to the hydrocarbons with the *trans* zig-zag conformation, the fluorocarbons take the helical conformation having nearly thirteen carbons per period. In the case of fluorinated comb polymers, if one assumed the uniaxial molecular orientation of the helical axes to the surface normal, the helix conformation of the fluorocarbon with C-F bonds tilted on the average 75.7° to its normal axis could be estimated in the film,[4,13,30,32] as indicated in the inset of Fig. 10,[9,10] The normalized intensity is given by:

$$R = \frac{B}{(1 - 3\sin^2\beta)B + 4\sin^2\beta}$$

$$B = 2\sin^2\theta + 2\sin^2\alpha - 3\sin^2\theta\sin^2\beta;$$

θ: incident angle, β: angle of refraction,

The orientation angle of the fluorinated side-chains was obtained by fitting the polarized dependence of the normalized peak intensity of σ^*(C–F) at 694 eV for the NEXAFS spectra to the angular dependence curves with the assumed molecular orientation.[30,31]

Results and Discussion

(1) Spectral Analysis and Comparison of Molecular Arrangements of X- and Z-type Monolayers for the F K-edge NEXAFS Spectra of Fluorinated Comb Polymer Films and Their Dependence on Chemical Structure. The NEXAFS spectra at the F K-edge and C K-edge for the fluorinated comb-polymer films were deconvoluted by fitting several Gaussian functions from the lower to the high photon energy and each

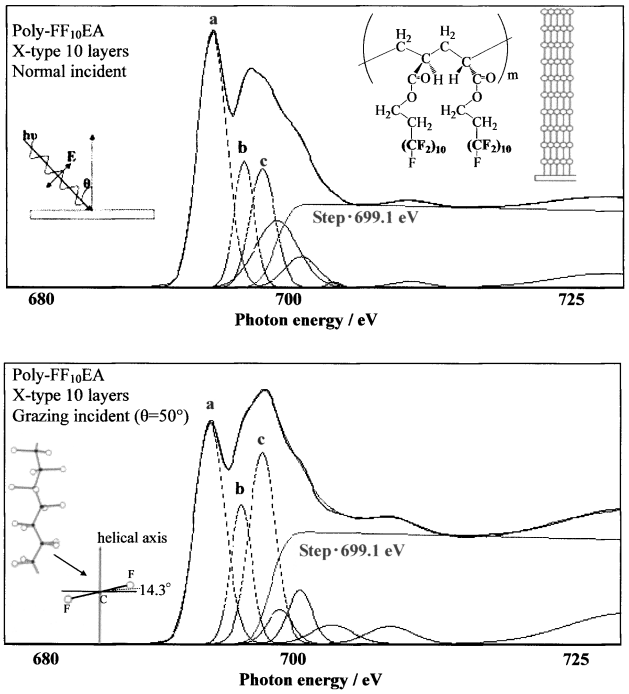

Peaks	Photon energy	Transition level from F1s
a	694.0 eV	σ*(C-F)
b	696.6 eV	σ*(C-F)
c	698.3 eV	σ*(C-C)

Fig. 1. Deconvolution of the F K-edge NEXAFS spectra for the X-type 10 layers of Poly-FF_{10}EA film and their assignments in the bottom.

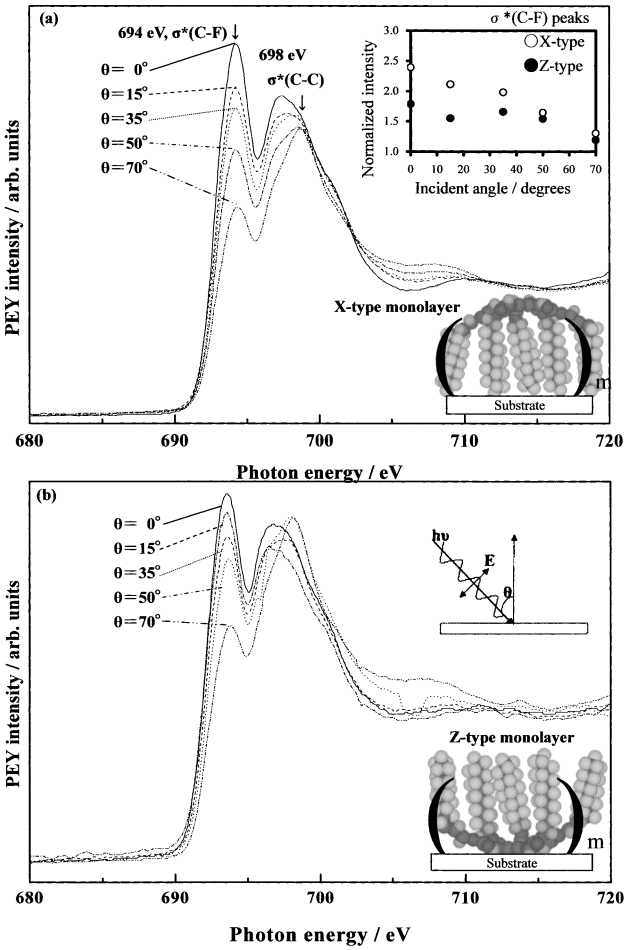

Fig. 2. Incident angle dependence of F K-edge NEXAFS spectra for (a) X- and (b) Z-type monolayers (25 mN m^{-1}, 5 °C) of Poly-FF_{10}EA on NESA glass substrate glass substrate. (inset Fig. 1(b)). Plots of the normalized 694 eV peak intensity vs. the incident angle, as indicated in the inset of Fig. 1(a).

band could be assigned by referring to the literature values. For examples, the F K-edge NEXAFS spectra for the X-type 10 layers of Poly-FF_{10}EA with the normal and grazing X-ray incidence could be assigned to transitions from the F1s level to the σ^*(C–F) and σ^*(C–C) levels at 694.0 & 696.6 eV and 698.3 & ~709 eV, respectively, as shown in Fig. 1 with the Table at the bottom. The symbol **E** means the electric vector. These assignments are consistent with the early work for evaporated films of perfluorotetracosane presented by Seki, et al.;[10] the assignments of peaks at higher energy region were made plausible by the curve fitting.

Figures 2(a) and (b) show the F K-edge NEXAFS spectra of the X-type and Z-type monomolecular layers for Poly-FF_{10}EA for various incidence angles. It is found that both spectra depend significantly upon the incidence angle at the monolayer level. The peaks at 694 and 698 eV have been assigned to the transitions from F1s to the σ^*(C–F) and σ^*(C–C) orbitals, respectively. The relative intensity of the σ^*(C–F) peak, attributable to the fluorocarbon side-chains, with respect to the σ^*(C–C) becomes maximum at normal incidence and weakened at grazing incidence ($\theta = 70°$) for both films. These results suggest that the transition moments of the 694 eV band were rather parallel to the surface, indicating the nearly perpendicular orientation of the fluorocarbons. Compared to the Z-type film, in which the fluorocarbon side-chains are exposed to air, the X-type film, in which the outermost surface consists of the polymer main-chains, produces a higher normalized σ^*(C–F) intensity, as shown in the inset of Fig. 2(a). It is therefore plausible that the uniformity of molecular alignments of the fluorocarbons in the outermost layers was degraded during or subsequent to the deposition, although the toughness of the polymer main-chain remained unchanged at the molecular level. Figure 3 shows the change in the NEXAFS spectra for the monomolecular films of fluorinated comb polymers with different α-substitutions of –H and $–CH_3$ at the hydrophilic polymer main-chains and with hydrogen (H) atoms instead of fluorine (F) atoms at the ω-position of the fluorocarbons. A clear angular dependence can be observed, suggestive of highly ordered molecular arrangements in the X-type monomolecular layers of Poly-FF_{10}EA, Poly-FF_{10}EMA, Poly-F_{10}A and Poly-F_{10}MA. All these films exhibited similar plots of the normalized 694 eV peak intensity versus the incident angle. The contribution of the σ^*(C–F) orbital (694 eV) attributable to fluorocarbon side-chains was largest at the normal incidence, whereas the σ^*(C–C) orbital (698 eV) became prominent at the grazing incidence. These results indicate that the fluorocarbon side-chains stand almost vertically and are anchored to the polymer

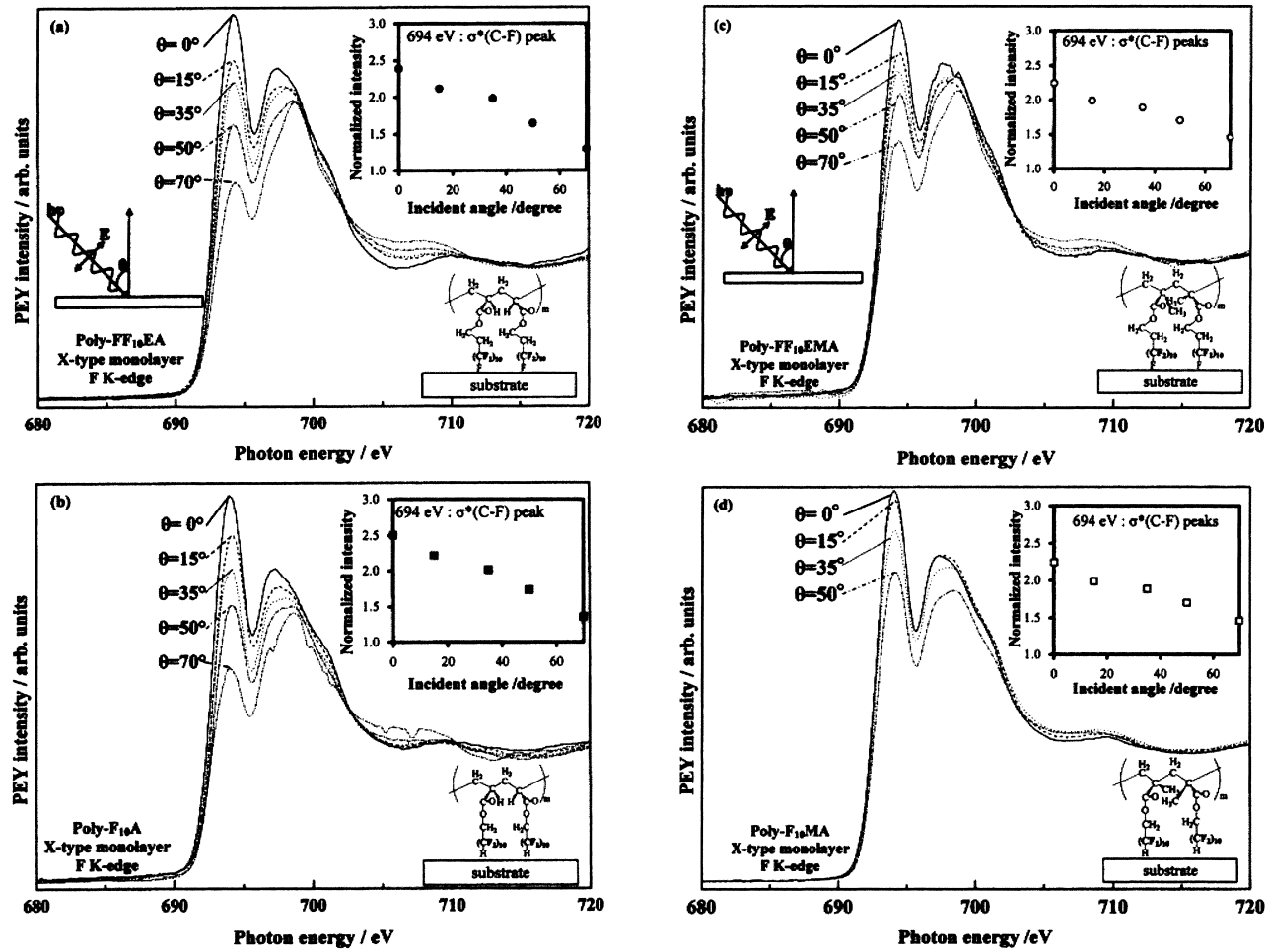

Fig. 3. Incident angle dependence of F K-edge polarized NEXAFS spectra for X-type monolayers (25 mN m^{-1}, 5 °C) of (a) Poly-FF_{10}EA, (b) Poly-F_{10}A, (c) Poly-FF_{10}EMA, and (d) Poly-F_{10}MA on NESA glass substrate. Plots of the normalized 694 eV peak intensity vs. the incident angle, as shown in the insets.

main-chains in the monolayers, irrespective of the chemical structures.

(2) C K-Edge NEXAFS Spectral Analysis and Structural Estimation for Mono- and Multilayers of the Fluorinated Comb Polymers. Figure 4 shows the deconvolution of the C *K*-edge NEXAFS spectra for the X-type 10 layers of Poly-FF_{10}EA with the normal and grazing X-ray incidence. The transition bands from the C1s level were assigned as listed in the bottom table. The three peaks at the lower energy region were assigned to transitions from the C1s to the σ^*(C–H) and π^*(C=O),[33–36] which could be considered without any contribution to the orientation of fluorocarbons. Figure 5 shows the C K-edge NEXAFS spectra for the X-type monomolecular comb polymers films with hydrogen atoms (Poly-F_{10}A) instead of fluorine atoms (Poly-FF_{10}EA) at the ω-positions of the fluorocarbon side-chains. The peaks at 293 and 296 eV can be assigned to the transitions from C1s to the σ^*(C–F) and σ^*(C–C) orbitals, respectively.[10] The relative intensity of the σ^*(C–F) peak, also attributable to the fluorocarbon side-chains, with respect to the σ^*(C–C) becomes maximum at normal incidence and weakened at the grazing incidence (θ = 70°) for both films. In these cases, a clear angular dependence can also be observed, suggestive of highly ordered molecular arrangements in the X-type monomolecular layers of both Poly-FF_{10}EA and Poly-F_{10}A, whereas the normalized C1s–σ^*(C–F) peak intensity of Poly-FF_{10}EA exhibited higher values as compared with those of Poly-F_{10}A. Since thresholds of the transition from C1s and F1s to the σ^*(C–F), σ^*(C–C), σ^*(C–H) and π^*(C=O) are different and the molecular orientation could not be estimated from the angular dependence of several peaks except for the C1S and F1S–σ^*(C–F) transitions due to uncertainty of peak positions, quantitative analysis of transition peaks based on the normalization by edge-jump can be done at C1S and F1S–σ^*(C–F) peaks only.

(3) Effects of Inter- and Intralayer Hydrogen Bonding on the Molecular Orientation in Organized Molecular Films of the Fluorinated Comb Polymers Having Hydrogen Atom at the ω-Position of the Side-Chains. Due to the effect of interlayer hydrogen bonding, subsequent layers of the comb polymers with hydrogen atoms at the ω-position of the side-chains of the fluorocarbons in multilayer films exhibited varying degrees of disorder. Figure 6 shows the F K-edge NEXAFS spectra for the X-type multilayer (10 layers) films of Poly-FF_{10}EA, Poly-FF_{10}EMA, Poly-F_{10}A and Poly-F_{10}MA. The structural information of the top few layers was obtained, taking into account the probing depth of the PEY mode.[9,10]

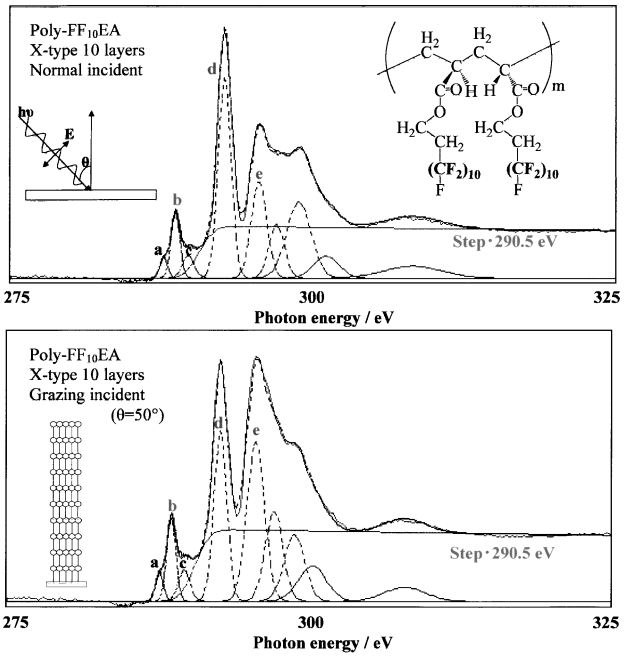

Peaks	Photon energy	Transition level from C1s
a	287.6 eV	σ*(C-H)
b	288.6 eV	π*(C=O)
c	289.6 eV	σ*(C-H)
d	292.6 eV	σ*(C-F)
e	295.6 eV	σ*(C-C)

Fig. 4. Deconvolution of the C K-edge NEXAFS spectra for the X-type 10 layers of Poly-FF_{10}EA film, and their assignments in the bottom.

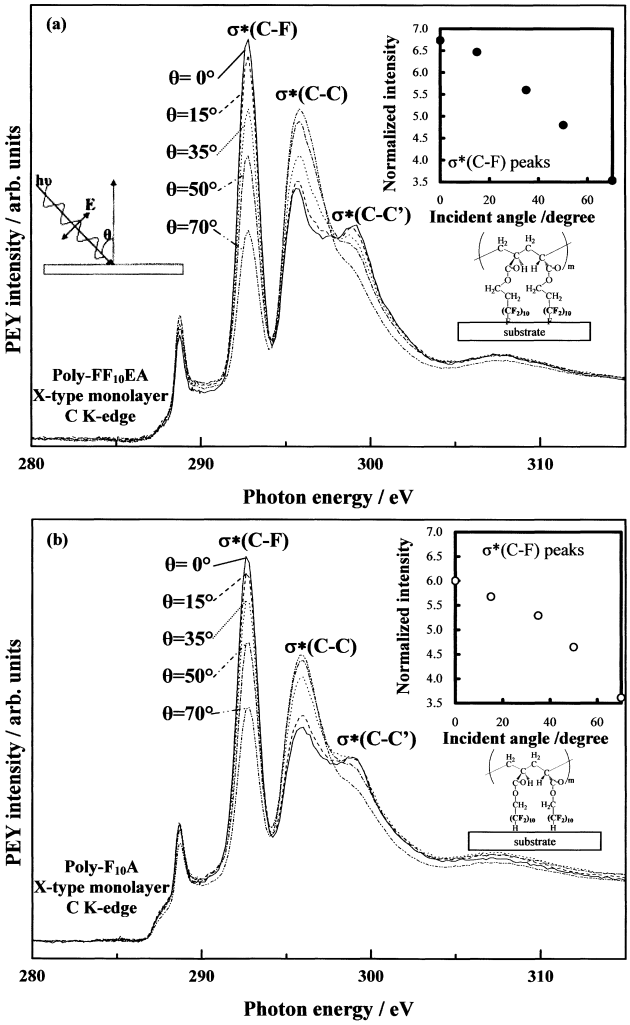

Fig. 5. Incident angle dependence of C K-edge polarized NEXAFS spectra for X-type monolayers (25 mN m^{-1}, 5 °C) of (a) Poly-FF_{10}EA and (b) Poly-F_{10}A on NESA glass substrate. Plots of the normalized 293 eV peak intensity vs. the incident angle, as shown in the insets.

Again, there is a clear variation with respect to the incidence angle. From the plots of normalized σ^*(C–F) intensity, the upper layers in the X-type multilayer films appear to be well-ordered. In particular, the multilayer Poly-FF_{10}EA and Poly-FF_{10}EMA films were more highly ordered than the monolayer films. However, the multilayer film of Poly-F_{10}A, having hydrogen atoms at the ω-position of the fluorocarbon side-chains, was notably disordered and the normalized intensity of the σ^*(C–F) peak remained constant irrespective of the incident angle.

Figure 7 shows the C K-edge NEXAFS spectra for the multilayers of comb polymers films with hydrogen (H) atoms instead of fluorine (F) atoms at the ω-position of the fluorocarbons. The multilayer film of Poly-F_{10}A, having hydrogen atoms at the ω-position of the fluorocarbon side-chains, no longer depended on the incident angle and the normalized intensity of the σ^*(C–F) peak remained constant irrespective of the incident angle.

Figure 8 shows the plots of the normalized intensity of the σ^*(C–F) peak on F K-edge polarized NEXAFS spectra vs. the incident angles, varying with the number of layers for the X-type films of Poly-FF_{10}EA and Poly-F_{10}A. For the Poly-FF_{10}EA film the increase of the normalized intensity with the number of layers was clearly observed, suggesting the well-ordered layer-structures due to formation of a crystalline-like packed molecular arrangements and with less influence for the surface roughness on the substrate. In the case of Poly-F_{10}A the above-mentioned angular dependence of the intensities was observed for the film below 6 layers, whereas the intensities were unchanged with the incident angles for the films above 8 layers. These facts indicate that the molecular ordered structures decreased gradually with the number of layers and that a random orientation of the molecules appeared in the films with more than 8 layers. This is probably due to the interlayer hydrogen bonding between ω-position hydrogen atoms and carbonyl groups of the Poly-F_{10}A film. The infrared spectra of these films suggested the hydrogen bonding from the shift of the $\nu_{C=O}$ bands from 1750 cm^{-1} (free of hydrogen bonding) to 1730 and below 1700 cm^{-1}.

The formation of the intralayer hydrogen bonding between ω-position hydrogen atoms and carbonyl groups was observed in the monolayer by the spreading from mixed solvents of CF_3COOH and *n*-hexane as the good and poor solvents, respectively,[19] Here the carbonyl band of the IR spectra for the Poly-F_{10}A film was shifted and split, and the surface morphol-

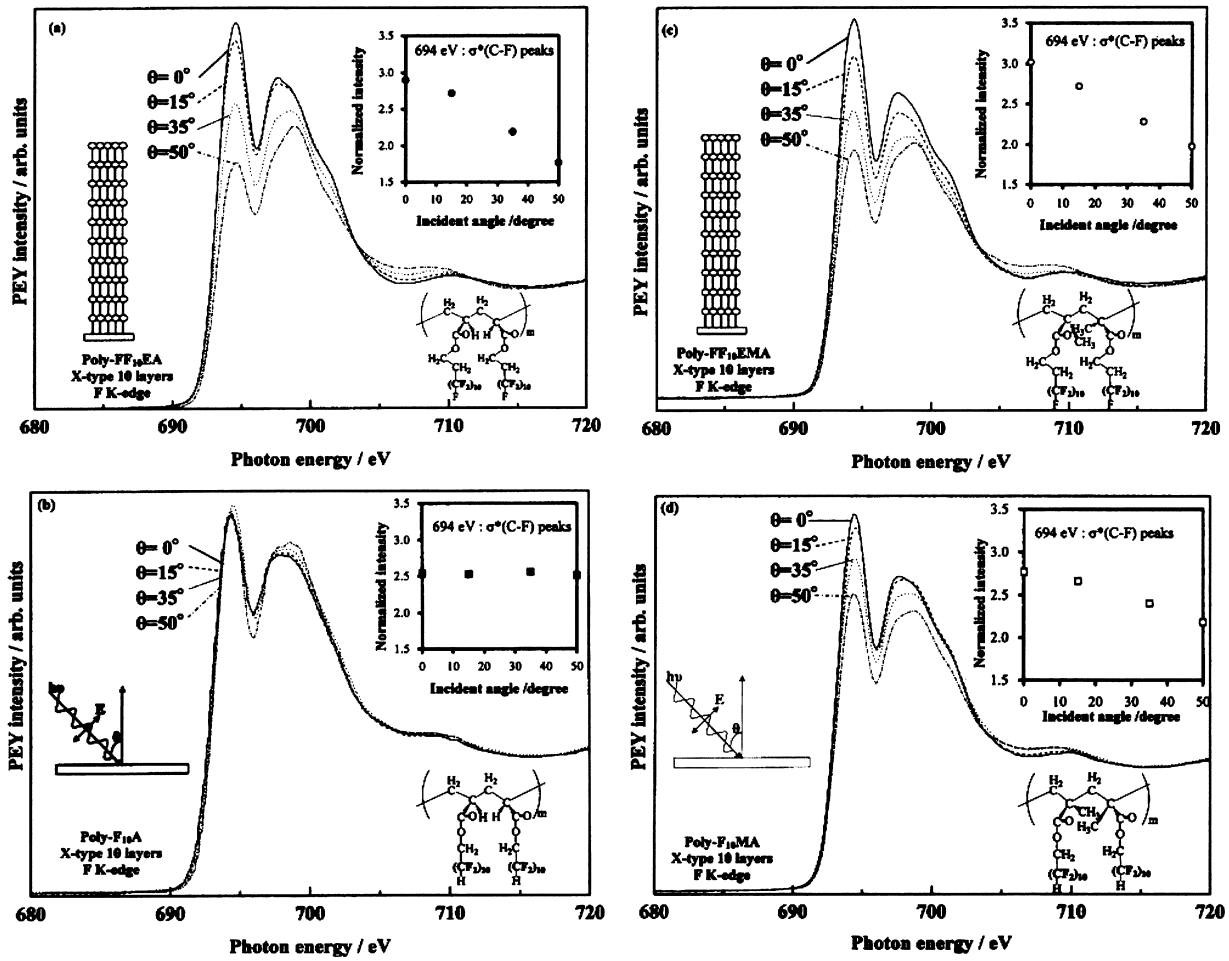

Fig. 6. Incident angle dependence of F K-edge polarized NEXAFS spectra for X-type multilayers (10 layers, 25 mN m^{-1}, 5 °C) of (a) Poly-FF_{10}EA, (b) Poly-F_{10}A, (c) Poly-FF_{10}EMA, and (d) Poly-F_{10}MA on NESA glass substrate. Plots of the normalized 694 eV peak intensity vs. the incident angle, as shown in the insets.

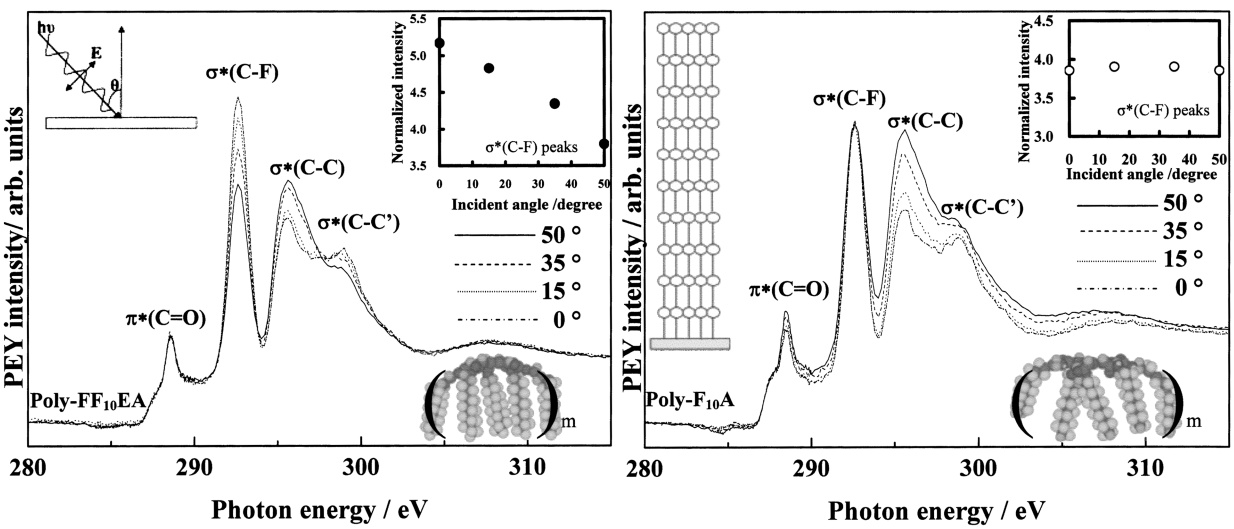

Fig. 7. Incident angle dependence of C K-edge polarized NEXAFS spectra for X-type multilayers (10 layers, 25 mN m^{-1}, 5 °C) of Poly-FF_{10}EA and Poly-F_{10}A on NESA glass substrate. Plots of the normalized 293 eV peak intensity vs. the incident angle, are shown in the insets.

ogy with clear irregular domains was observed by Brewster angle, scanning electron, and atomic force microscopies. In

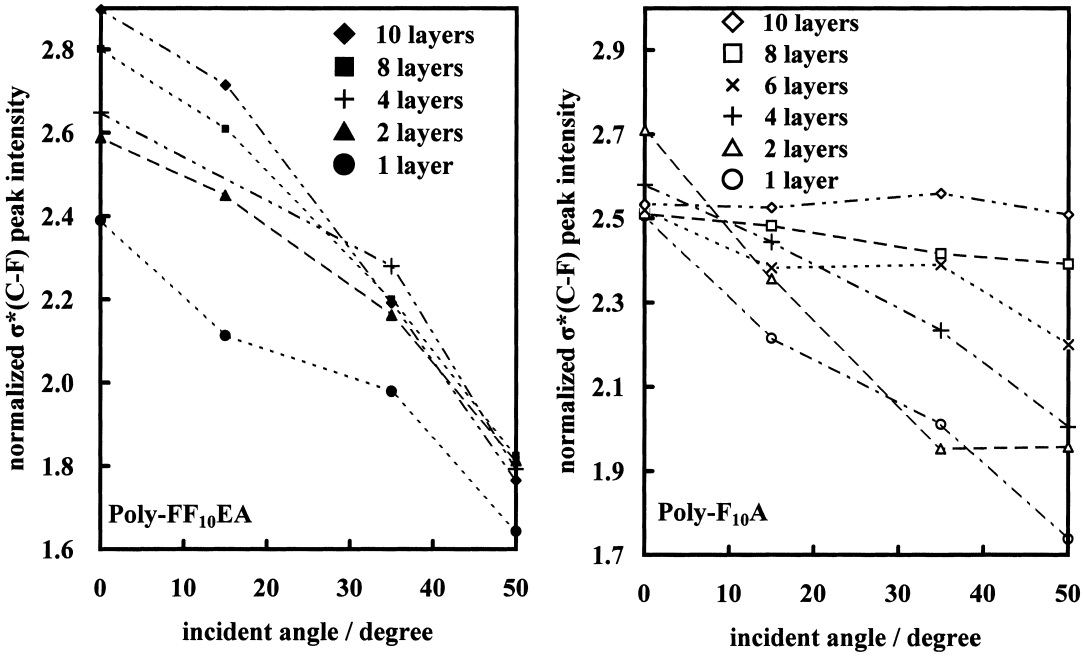

Fig. 8. Dependence for the number of layers on F K-edge polarized NEXAFS spectra of multilayers for Poly-FF_{10}EA and Poly-F_{10}A.

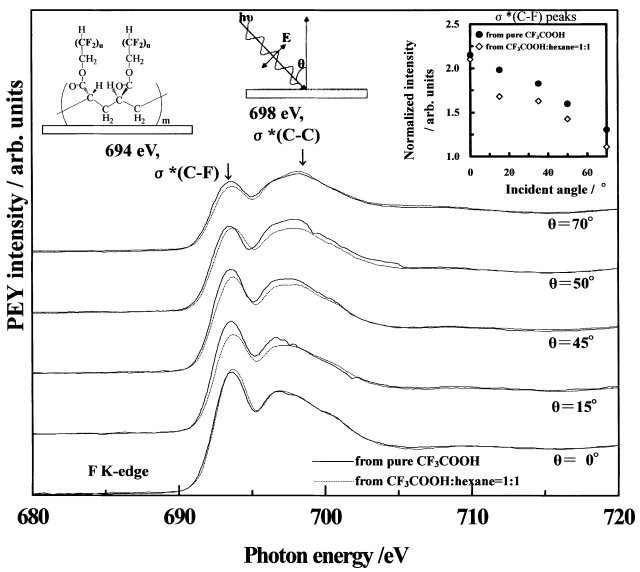

Fig. 9. Polarized NEXAFS spectra of Poly-F_{10}A Z-type monolayers spread from CF_3COOH and the mixed solvents with *n*-hexane (1:1, v/v). Plots of the normalized 694 eV peak intensity vs. the incident angle, as shown in the inset.

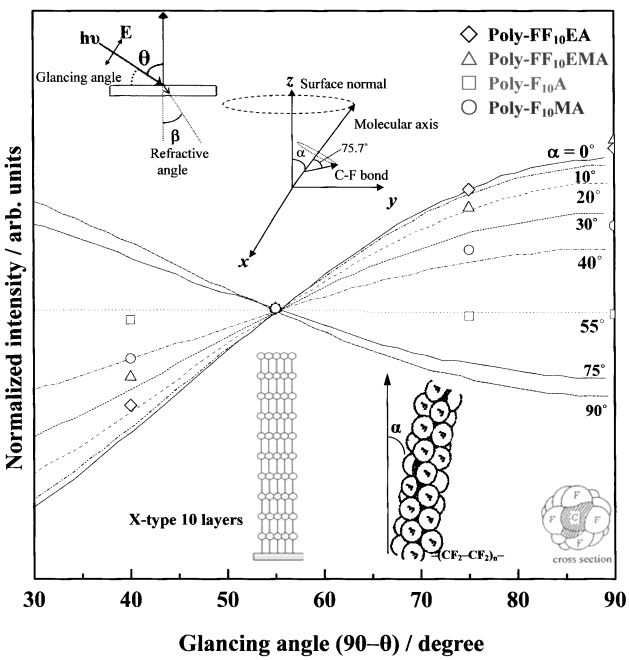

Fig. 10. Plots of the normalized σ^*(C–F) peaks of NEXAFS spectra vs the incident angle for various molecular orientations assumed by the uniaxial in the X-type 10 layers of the fluorinated comb polymers.

order to support these results, the change of molecular arrangements in the several monolayers was also examined by polarized F K-edge NEXAFS spectroscopy. Figure 9 shows the dependence of the incidence angle on the F K-edge NEXAFS spectra of the transferred Z-type monomolecular layer on NESA glass at 15 mN m^{-1} for Poly-F_{10}A spread from the trifluoroacetic acid:*n*-hexane = 1:1 mixed solution, indicating the well-ordered molecular orientation of the fluorinated comb polymer in this monolayer. The fluorocarbon side-chains have a slight tendency of random alignments, accompanied with addition of the poor solvent into the spreading solution on the monolayer level resolution.

(4) Estimation of the Orientation Angles for the X-Type 10 Layers of Fluorinated Comb Polymers. Figure 10 shows the estimation of the orientation angle for Poly-FF_{10}EA, Poly-FF_{10}EMA, Poly-F_{10}A and Poly-F_{10}MA molecules in the

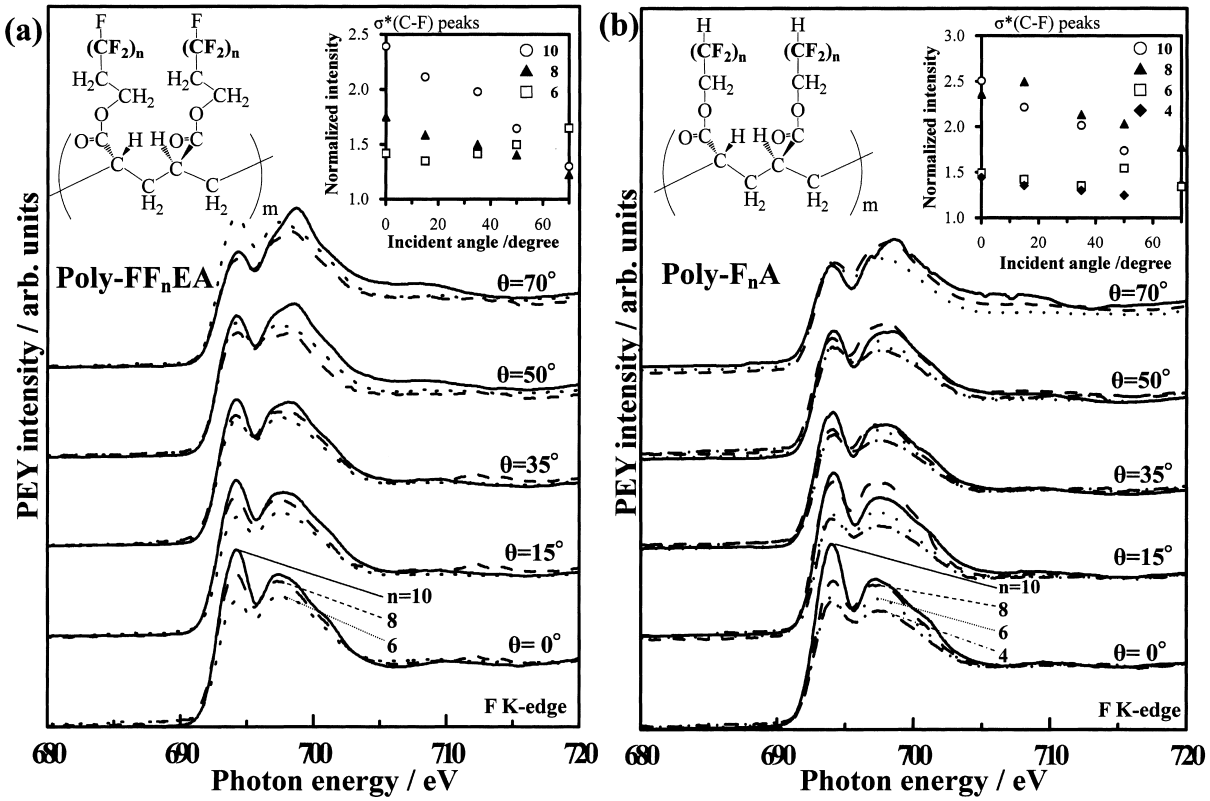

Fig. 11. Incident angle dependence of F K-edge NEXAFS spectra for monolayers of (a) Poly-FF$_n$EA (n = 6, 8, 10), and (b) Poly-F$_n$A (n = 4, 6, 8, 10) with various side-chain lengths of the fluorocarbons on NESA glass substrate. Plots of the normalized 694 eV peak intensity vs the incident angle, are shown in the insets.

X-type 10 layers from the polarized F *K*-edge NEXAFS spectra. Assuming the uniaxial molecular orientation in the film and taking the tilted angle 14.3° of the $-CF_2$ plane to the perpendicular direction of the molecular axis of the fluorocarbon, we determined the orientation angles of the fluorinated side-chain by comparison of the polarized dependence of the normalized peak intensity for the NEXAFS spectra and the ideal orientation angular curves. These results show that the fluorocarbons of Poly-FF$_{10}$EA are in almost perpendicular orientation to the surface. This result agreed clearly with the value estimated by the previous X-ray diffraction study.[19] Poly-F$_{10}$A were apparently orientated at the magic angle or showed little polarization dependence due to a random conformation. This figure indicated also the orientation of the fluorocarbons of Poly-FF$_{10}$EMA and Poly-F$_{10}$MA molecules in the transferred films, and those are found to be tilted about 20° or 40° to the surface normal. This lack of dependence of the incidence angles i.e., the glancing angles on the normalized intensities of the side-chains of Poly-F$_{10}$A and Poly-F$_{10}$MA can be ascribed to some random orientation in the films due to the hydrogen bonding.

(5) Dependence of the Side-Chain Length on the Structures of the Molecular Assemblies of the Comb Polymers. In the case of various lengths (n) of the fluorocarbon side-chains for the comb polymers of Poly-FF$_n$EA and Poly-F$_n$A, the angular dependence of the F K-edge NEXAFS spectra for X-type monolayers are shown in Fig. 11. No clear change of the normalized intensity of the σ^*(C–F) peak at 694 eV with the incident angles could be observed for the films with n = 4 and 6, suggesting that the comb polymers with the shorter fluorocarbon side-chains below n = 6 form random conformations of the fluorocarbons in the films. The σ^*(C–C) bands at 698 eV in the spectra changed slightly with the incident angle, reflecting any different conformations and inductive effects of the fluorocarbons. Although molecular orbital and band calculations have been employed in the previous studies in an attempt to interpret features in the high-energy region of NEXAFS spectra,[9,10] the high-energy bands observed in the present study are not readily interpretable.

Conclusion

The angular dependence of the incident X-ray on the NEXAFS spectra for the organized molecular films of fluorinated comb polymers on solids gives very useful information on the orientation of the fluorocarbon side-chains of those polymers. Minor changes in the chemical structure of fluorinated comb polymers, such as changing the α-methyl substituents on the polymer backbones and substituting the hydrogen atoms instead of the fluorine at the ω-position of the fluorocarbons, were found to affect significantly the polarization dependence of NEXAFS spectra of the transferred films. The hydrogen substitution at the ω-position of the fluorocarbons is considered to allow the formation of hydrogen bonds with the carbonyl groups of the esters and to distort the molecular orientation in the comb polymer films. The NEXAFS spectra, clearly related to the uniformity of the molecular orientation in

the films, were also observed to vary according to the film type (X or Z) and the number of layers in the multilayer films as well as the fluorocarbon side-chain length.

The authors thank Drs. Yoshinori Kitajima, KEK-PF, and Kenta Amemiya, Univ. of Tokyo for their help of NEXAFS measurements and helpful discussion. One of authors (A. F.) thanks the Japan Society for Promotion of Science for a post-doctoral fellowship. This work was performed under approval of the Photon Factory Program Advisory Committee (proposal No. 2000G282).

References

1 H. I. Kim, T. Koini, T. R. Lee, and S. S. Perry, *Langmuir*, **13**, 7192 (1997).

2 T. Ohzono, J. N. Glosli, and M. Fujihira, *Jpn. J. Appl. Phys.*, **37**, 6535 (1998).

3 "Fluoropolymers 2," ed by G. Hougham et al., in "Topics in Applied Chemistry," Kluwer Acad./Plenum Pub., New York (1999).

4 C. W. Bunn and E. R. Howells, *Nature*, **18**, 549 (1954).

5 J. Schneider, C. Erdelen, H. Ringsdorf, and H. Rabolt, *Macromolecules*, **22**, 3475 (1989).

6 A. Fujimori, T. Araki, and H. Nakahara, *Chem. Lett.*, **2000**, 898.

7 A. Fujimori, T. Araki, H. Nakahara, E. Ito, M. Hara, H. Ishii, Y. Ouchi, and K. Seki, *Chem. Phys. Lett.*, **349**, 6 (2001).

8 A. Fujimori, T. Araki, and H. Nakahara, *J. Colloid Interface Sci.*, **247**, 351 (2002).

9 J. Stöhr, "NEXAFS Spectroscopy," Springer, Berlin (1992).

10 K. Seki, R. Matsumoto, E. Ito, T. Araki, T. Sakurai, D. Yoshimura, H. Ishii, Y. Ouchi, T. Miyamae, T. Narita, S. Nishimura, Y. Takata, T. Yokoyama, T. Ohta, S. Suganuma, F. Okino, and H. Touhara, *Mol. Cryst. Liq. Cryst.*, **355**, 247 (2001).

11 D. A. Outka, J. Stöhr, J. P. Rabe, and J. Swalen, *J. Chem. Phys.*, **88**, 4076 (1988).

12 K. Seki, T. Yokoyama, T. Ohta, H. Nakahara, and K. Fukuda, *Mol. Cryst. Liq. Cryst.*, **218**, 609 (1992).

13 T. Ohta, K. Seki, T. Yokoyama, I. Morisada, and K. Edamatsu, *Phys. Scripta*, **41**, 150 (1990).

14 Ch. Ziegler, Th. S. Niedrig, G. Beamson, D. T. Clark, W. R. Salaneck, H. Sotobayashi, and A. M. Bradshaw, *Langmuir*, **10**, 4399 (1994).

15 K. Nagayama, R. Mitsumoto, T. Araki, Y. Ouchi, and K. Seki, *Physica B*, **208/209**, 419 (1995).

16 L. G. Gamble, B. Ravel, D. A. Fischer, and D. G. Castner, *Langmuir*, **18**, 2183 (2002).

17 H. Kondoh, F. Matsui, Y. Ehara, T. Yokoyama, and T. Ohta, *Langmuir*, **17**, 8178 (2001).

18 R. D. Peters, P. F. Nealey, J. N. Crain, and F. J. Himpsel, *Langmuir*, **18**, 1250 (2002).

19 Y. Mo, I. C. Stefan, W. Cai, J. Dong, P. Carey, and D. A. Scherson, *J. Phys. Chem. B*, **106**, 3681 (2002).

20 A. Fujimori, T. Araki, H. Nakahara, E. Ito, M. Hara, H. Ishii, Y. Ouchi, and K. Seki, *Langmuir*, **18**, 1437 (2002).

21 Y. Shibasaki, H. Saitoh, and K. Chiba, *J. Thermal Anal.*, **49**, 115 (1997).

22 A. Fujimori, H. Saitoh, and Y. Shibasaki, *J. Thermal Anal.*, **57**, 631 (1999).

23 K. Yamada, T. Nakano, and Y. Okamoto, *Polymer J.*, **30**, 641 (1998).

24 H. J. Trurnit, *J. Colloid Sci.*, **15**, 1 (1960).

25 K. Fukuda, H. Nakahara, and T. Kato, *J. Colloid and Interface Sci.*, **54**, 430 (1976).

26 H. E. Ries, *J. Colloid Sci.*, **16**, 361 (1961).

27 K. Amemiya, Y. Kitajima, T. Ohta, and K. Ito, *J. Synchrotron Rad.*, **3**, 282 (1996).

28 Y. Kitajima, Y. Yokoyama, K. Amemiya, H. Tsukabayashi, T. Ohta, and K. Ito, *J. Elec. Spectrosc. Relat. Phenom.*, **927**, 101 (1999).

29 K. K. Okudaira, H. Yamane, K. Ito, M. Imamura, S. Hasegawa, and N. Ueno, *Surf. Rev. Lett.*, **9**, 335 (2002).

30 H. Akutsu, Y. Kyogoku, H. Nakahara, and K. Fukuda, *Chem. Phys. Lipids*, **15**, 222 (1975).

31 K. Matsuki, Y. Nagahira, H. Fukutome, *Bull. Chem. Soc. Jpn.*, **53**, 1817 (1980).

32 N. Yoshino and Y. Kondo, *Jpn. J. Oil. Chem.*, **49**, 1081 (2000).

33 J. Stöhr and D. A. Outka, *Am. Phys. Soc.*, **36**, 7891 (1987).

34 D. A. Outka, J. Stöhr, R. J. Madix, H. H. Rotermund, B. Hermsmeier, and J. Solomon, *Surf. Sci.*, **53**, 185 (1987).

35 Y. Ouchi, I. Mori, M. Seki, E. Ito, T. Araki, H. Ishii, K. Seki, and K. Kudo, *Physica B*, **208/209**, 407 (1995).

36 J. A. Horsly, J. Stöhr, A. P. Hitchcock, D. C. Newbury, A. L. Johnson, F. Sette, *J. Chem. Phys.*, **83**, 6099 (1985).